



**Defense Threat Reduction Agency  
8725 John J. Kingman Road, MS-6201  
Fort Belvoir, VA 22060-6201**



**DTRA-TR-17-019 (R1)**

# **TECHNICAL REPORT**

## **Utilization of ICU Data to Improve 30 and 60-Day HENRE Mortality Models, Revision 1**

DISTRIBUTION A. Approved for public release; distribution is unlimited.

May 2017

HDTRA1-14-D-0003; 0005

Prepared by:

Applied Research Associates, Inc.  
801 N. Quincy Street  
Suite 700  
Arlington, VA 22203

**REPORT DOCUMENTATION PAGE**

*Form Approved  
OMB No. 0704-0188*

The public reporting burden for this collection of information is estimated to average 1 hour per response, including the time for reviewing instructions, searching existing data sources, gathering and maintaining the data needed, and completing and reviewing the collection of information. Send comments regarding this burden estimate or any other aspect of this collection of information, including suggestions for reducing the burden, to Department of Defense, Washington Headquarters Services, Directorate for Information Operations and Reports (0704-0188), 1215 Jefferson Davis Highway, Suite 1204, Arlington, VA 22202-4302. Respondents should be aware that notwithstanding any other provision of law, no person shall be subject to any penalty for failing to comply with a collection of information if it does not display a currently valid OMB control number.

**PLEASE DO NOT RETURN YOUR FORM TO THE ABOVE ADDRESS.**

1. REPORT DATE (DD-MM-YYYY) 12-05-2017	2. REPORT TYPE Technical Report	3. DATES COVERED (From - To)
---	------------------------------------	------------------------------

4. TITLE AND SUBTITLE Utilization of ICU Data to Improve 30 and 60-Day HENRE Mortality Models, Revision 1	5a. CONTRACT NUMBER HDTRA1-14-D-0003/0005
	5b. GRANT NUMBER
	5c. PROGRAM ELEMENT NUMBER

6. AUTHOR(S) Bellman, Jacob Pirone, Jason Crary, Dave Beaulieu, Stephen	5d. PROJECT NUMBER
	5e. TASK NUMBER
	5f. WORK UNIT NUMBER

7. PERFORMING ORGANIZATION NAME(S) AND ADDRESS(ES) Applied Research Associates, Inc. 801 N. Quincy Street, Suite 700 Arlington, VA 22203	8. PERFORMING ORGANIZATION REPORT NUMBER
---	--

9. SPONSORING/MONITORING AGENCY NAME(S) AND ADDRESS(ES) Nuclear Technologies Department, Attn: Dr. Blake Defense Threat Reduction Agency 8725 John J. Kingman Road, Mail Stop 6201 Fort Belvoir, VA 22060-6201	10. SPONSOR/MONITOR'S ACRONYM(S) DTRA J9NTSN
	11. SPONSOR/MONITOR'S REPORT NUMBER(S) DTRA-TR-17-019 (R1)

12. DISTRIBUTION/AVAILABILITY STATEMENT DISTRIBUTION A. Approved for public release: distribution is unlimited.
--

13. SUPPLEMENTARY NOTES
-------------------------

14. ABSTRACT This report presents the use of available ICU data to extend the capabilities of 30 and 60-day mortality models in the Health Effects from Nuclear and Radiological Environments (HENRE) software. These models relate levels of molecular and cellular biomarkers currently modeled in HENRE to mortality using data from the medical literature. A small intestine injury model predicts the probability of 30-day mortality after radiation and burn combined injuries using the biomarker citrulline, and a platelet reduction model predicts the probability of 60-day mortality after burn. These models have been developed to predict mortality of casualties with access to standard medical care. A review of the literature on the use of the neutrophil to lymphocyte ratio (NLR) as a biomarker of inflammation and mortality is presented. The NLR may be used in future work to further extend the capabilities of the mortality models in HENRE.
--

15. SUBJECT TERMS Acute Radiation Syndrome, Mortality, Burn Combined Injury, Lethality, Small Intestine, Ordinary Differential Equations Model, Thrombopoiesis, Granulopoiesis, Lymphopoiesis
--

16. SECURITY CLASSIFICATION OF:			17. LIMITATION OF ABSTRACT	18. NUMBER OF PAGES 41	19a. NAME OF RESPONSIBLE PERSON Dr. Paul Blake, Ph.D.
a. REPORT U	b. ABSTRACT U	c. THIS PAGE U			19b. TELEPHONE NUMBER (Include area code) 703-767-3433

## UNIT CONVERSION TABLE

U.S. customary units to and from international units of measurement\*

U.S. Customary Units	Multiply by Divide by <sup>†</sup>	International Units
<b>Length/Area/Volume</b>		
inch (in)	2.54 × 10 <sup>-2</sup>	meter (m)
foot (ft)	3.048 × 10 <sup>-1</sup>	meter (m)
yard (yd)	9.144 × 10 <sup>-1</sup>	meter (m)
mile (mi, international)	1.609 344 × 10 <sup>3</sup>	meter (m)
mile (nmi, nautical, U.S.)	1.852 × 10 <sup>3</sup>	meter (m)
barn (b)	1 × 10 <sup>-28</sup>	square meter (m <sup>2</sup> )
gallon (gal, U.S. liquid)	3.785 412 × 10 <sup>-3</sup>	cubic meter (m <sup>3</sup> )
cubic foot (ft <sup>3</sup> )	2.831 685 × 10 <sup>-2</sup>	cubic meter (m <sup>3</sup> )
<b>Mass/Density</b>		
pound (lb)	4.535 924 × 10 <sup>-1</sup>	kilogram (kg)
atomic mass unit (AMU)	1.660 539 × 10 <sup>-27</sup>	kilogram (kg)
pound-mass per cubic foot (lb ft <sup>-3</sup> )	1.601 846 × 10 <sup>1</sup>	kilogram per cubic meter (kg m <sup>-3</sup> )
Pound-force (lbf avoirdupois)	4.448 222	Newton (N)
<b>Energy/Work/Power</b>		
electron volt (eV)	1.602 177 × 10 <sup>-19</sup>	joule (J)
erg	1 × 10 <sup>-7</sup>	joule (J)
kiloton (kT) (TNT equivalent)	4.184 × 10 <sup>12</sup>	joule (J)
British thermal unit (Btu) (thermochemical)	1.054 350 × 10 <sup>3</sup>	joule (J)
foot-pound-force (ft lbf)	1.355 818	joule (J)
calorie (cal) (thermochemical)	4.184	joule (J)
<b>Pressure</b>		
atmosphere (atm)	1.013 250 × 10 <sup>5</sup>	pascal (Pa)
pound force per square inch (psi)	6.984 757 × 10 <sup>3</sup>	pascal (Pa)
<b>Temperature</b>		
degree Fahrenheit (°F)	[T(°F) - 32]/1.8	degree Celsius (°C)
degree Fahrenheit (°F)	[T(°F) + 459.67]/1.8	kelvin (K)
<b>Radiation</b>		
activity of radionuclides [curie (Ci)]	3.7 × 10 <sup>10</sup>	per second (s <sup>-1‡</sup> )
air exposure [roentgen (R)]	2.579 760 × 10 <sup>-4</sup>	coulomb per kilogram (C kg <sup>-1</sup> )
absorbed dose (rad)	1 × 10 <sup>-2</sup>	joule per kilogram (J kg <sup>-1§</sup> )
equivalent and effective dose (rem)	1 × 10 <sup>-2</sup>	joule per kilogram (J kg <sup>-1**</sup> )

\* Specific details regarding the implementation of SI units may be viewed at <http://www.bipm.org/en/si/>.

<sup>†</sup> Multiply the U.S. customary unit by the factor to get the international unit. Divide the international unit by the factor to get the U.S. customary unit.

<sup>‡</sup> The special name for the SI unit of the activity of a radionuclide is the becquerel (Bq). (1 Bq = 1 s<sup>-1</sup>).

<sup>§</sup> The special name for the SI unit of absorbed dose is the gray (Gy). (1 Gy = 1 J kg<sup>-1</sup>).

\*\* The special name for the SI unit of equivalent and effective dose is the sievert (Sv). (1 Sv = 1 J kg<sup>-1</sup>).

This page is intentionally left blank.

# Table of Contents

<b>Table of Contents</b> . . . . .	<b>i</b>
<b>List of Figures</b> . . . . .	<b>ii</b>
<b>List of Tables</b> . . . . .	<b>iii</b>
<b>Acknowledgements</b> . . . . .	<b>iv</b>
<b>Executive Summary</b> . . . . .	<b>1</b>
<b>1 Introduction</b> . . . . .	<b>2</b>
<b>2 Purpose</b> . . . . .	<b>4</b>
<b>3 Background</b> . . . . .	<b>5</b>
<b>4 Methods</b> . . . . .	<b>6</b>
4.1 Small Intestine Damage as a Predictor of 30-Day Mortality . . . . .	6
4.1.1 Background . . . . .	6
4.1.2 30-Day Mortality . . . . .	9
4.2 Platelet Levels as a Predictor of 60-Day Mortality . . . . .	10
4.2.1 Background . . . . .	10
4.2.2 60-Day Mortality . . . . .	13
4.3 Neutrophil to Lymphocyte Ratio . . . . .	14
4.3.1 Background . . . . .	14
4.3.2 NLR Studies . . . . .	15
<b>5 Results</b> . . . . .	<b>21</b>
<b>6 Discussion</b> . . . . .	<b>23</b>
<b>7 Future Work</b> . . . . .	<b>25</b>
<b>References</b> . . . . .	<b>26</b>
<b>8 Abbreviations, Acronyms and Symbols</b> . . . . .	<b>31</b>
<b>Appendix A Small Intestine Model Update</b> . . . . .	<b>32</b>

# List of Figures

1.1	Modeling capabilities of HENRE. . . . .	3
2.1	Mortality models based on small intestine and thrombocyte cell kinetics. . . . .	4
4.1	Small intestine cell kinetic model. . . . .	7
4.2	Small intestine combined injury example. . . . .	8
4.3	30-Day probability of mortality predicted from citrulline nadir. . . . .	9
4.4	Thrombopoiesis cell kinetic model. . . . .	11
4.5	Platelet counts of a burn patient. . . . .	12
4.6	60-Day probability of mortality predicted from platelet nadir. . . . .	13
4.7	Interactions of tissue injury with physiological and immunological disturbances that lead to post-injury morbidity and mortality (Valparaiso et al., 2015). . . . .	15
4.8	Activation of the inflammatory response in response to trauma, tissue damage, and infection (Lord et al., 2014). . . . .	16
4.9	Receiver operating characteristic curve of NLR to predict mortality (Akilli et al., 2014). . . . .	17
4.10	Kaplan-Meier survival curves for NLR quartiles determined in Akilli et al., 2014. . . . .	18
4.11	Kaplan-Meier survival curves for 1-year mortality based on NLR quartiles determined in Saliccioli et al., 2015. . . . .	19
4.12	ROC curves for (A) the NLR on hospital day 2 and (B) hospital day 5 (Dilektasli et al., 2016). . . . .	19
4.13	Kaplan Meier survival curves for (A) the day 2 cutoff of 8.19 and (B) the day 2 cutoff of 7.92 (Dilektasli et al., 2016). . . . .	20
5.1	Probability of 30-day mortality predicted by the SIMM. . . . .	21
5.2	Probability of 60-day mortality predicted from platelet reduction. . . . .	22
6.1	Domain of applicability for the small intestine and platelet mortality models. . . . .	24
A.1	Small intestine combined injury villus response with updated burn parameters (Table A.1). . . . .	33

# List of Tables

A.1 Biological descriptions, parameters and variables for burn response in the small intestine mathematical model. . . . .	32
--	----

## Acknowledgements

The authors of this modeling work acknowledge the technical developments by Dr. Olga Smirnova, who dedicated years of research and modeling efforts to develop the original structure for the cell kinetic models in this research, and the many experimentalists who collected the data that has been crucial for this modeling effort. We would also like to acknowledge Dr. John Gilstad and Dr. Glen Reeves for their invaluable feedback in reviewing this report. Finally, we gratefully acknowledge Dr. Paul Blake of DTRA/J9 for programmatic support. The work was performed under DTRA contract HDTRA1-14-D-0003; 005.

# Executive Summary

This report presents models based on biomarker data associated with small intestine epithelial kinetics and thrombopoiesis to predict mortality. These models improve the capabilities of the 30 and 60-day mortality models in HENRE by providing:

- The Small Intestine Mortality Model (SIMM) that uses small intestine epithelial cell kinetics and the amino acid biomarker, citrulline, to predict 30-day mortality. This model predicts the probability of mortality of an individual receiving treatment after being exposed to combined radiation and burn injury.
- The Platelet Attenuation Mortality Model (PAMM) that simulates thrombocyte cell kinetics to predict 60-day mortality. This model currently predicts the probability of mortality of an individual receiving treatment after being exposed to a burn injury. Lethality of radiation and combined injuries is not yet predicted with this model, although this is a goal for the future.

This report also provides a comprehensive literature review of the neutrophil to lymphocyte ratio (NLR), a biomarker of inflammatory response that describes the potential predictive power of the NLR for various health effects, including mortality. We will discuss the benefits of including an NLR-based mortality model with DTRA and, as appropriate, develop options for a future version of HENRE.

# 1 Introduction

Applied Research Associates (ARA) has been tasked by the Defense Threat Reduction Agency (DTRA) to support their mission to safeguard the United States against weapons of mass destruction (WMD). ARA is supporting this effort by developing state-of-the-art mathematical models that predict health effects and provide risk assessment of individuals exposed to harmful environments produced by a nuclear weapon. These models are built into DTRA's Health Effects from Nuclear and Radiological Environments (HENRE) modeling software. A crucial capability of HENRE is to predict lethality of various combinations of radiation, thermal, and blast insults.

In the event of an improvised nuclear device (IND) detonation, there would be a broad spectrum of casualties with various types of injuries. Probability of mortality for each individual will vary by the degree of exposure to radiation, burn and blast environments and the availability of medical treatment. In order to estimate mortality for this type of scenario, ARA is developing models to estimate 48-hour, 30-day, and 60-day mortality, as well as models to estimate serious injury as a function of time and exposure.

There are limitations for each of the mortality models currently in HENRE. For instance, the 30-day mortality model only accepts burn insults, and assumes the casualty receives no treatment following exposure (Stricklin, 2013a). The 60-day mortality model estimates the probability of mortality following a combined radiation and burn insult (Stricklin, 2013b). When radiation is the only insult provided, this model predicts mortality based on age, gender and available medical treatment (Stricklin, 2016). However, when burn is included, this model does not consider individual demographic differences, and only predicts mortality under the assumption that medical treatment is unavailable. A comprehensive list of lethality models in the latest version of HENRE are reviewed in detail in Oldson et al., 2015 and Stricklin, 2015.

The majority of the models previously developed for HENRE have assumed that a casualty receives no treatment. In this report, ICU data is used to develop models representative of casualties receiving standard care. The Small Intestine Mortality Model (SIMM) and the Platelet Attenuation Mortality Model (PAMM), both introduced in this report, are shown in the shaded cells of Figure 1.1. In this diagram, check marks represent available capabilities of HENRE, and empty squares represent scenarios that will be modeled in the future.

No Treatment				Standard Care			
<b>Radiation</b>	✓		✓	<b>Radiation</b>		<i>Small Intestine Mortality Model</i>	✓
<b>Thermal Burn</b>	✓	✓	✓	<b>Thermal Burn</b>		<i>Small Intestine Mortality Model</i>	<i>Platelet Attenuation Mortality Model</i>
<b>Trauma</b>	✓			<b>Trauma</b>			
	<b>48-Hour Mortality</b>	<b>30-Day Mortality</b>	<b>60-Day Mortality</b>		<b>48-Hour Mortality</b>	<b>30-Day Mortality</b>	<b>60-Day Mortality</b>

Figure 1.1: Modeling capabilities of HENRE.

## 2 Purpose

To improve the predictive capabilities of the mortality models in HENRE, we developed models to supplement the 30 and 60-day combined injury mortality models. The new version of the 30-day lethality model (SIMM) couples the small intestine cell kinetics model with a biomarker (citrulline) to predict mortality due to the combined effects of radiation and thermal injury. The new version of the 60-day lethality model (PAMM) uses the thrombocyte cell kinetic model to simulate a biomarker (platelets) to predict 60-day mortality as a function of burn size. The new models (SIMM and PAMM) were developed using intensive care unit (ICU) patient data to represent the standard care scenario shown in Figure 1.1. Figure 2.1 illustrates the overall structure of the two mortality models presented in this report.

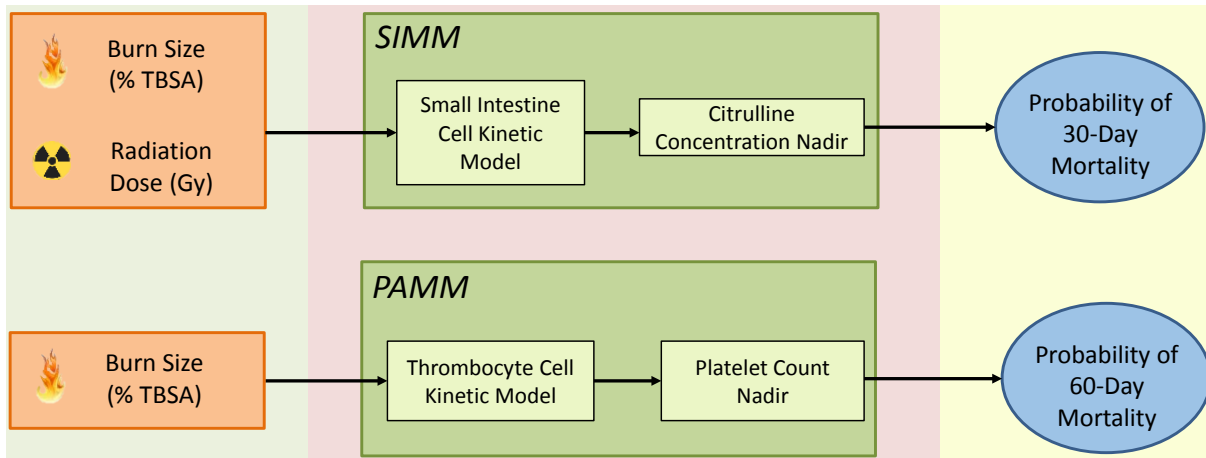


Figure 2.1: Mortality models based on small intestine and thrombocyte cell kinetics.

### 3 Background

Exposure to a large dose of radiation in a short period of time (high dose rate) causes acute radiation syndrome (ARS). Depending on the radiation dose, an individual may experience the hematopoietic acute radiation syndrome (H-ARS) or the gastrointestinal acute radiation syndrome (GI-ARS) (reviewed in Macià I Garau et al., 2011). For acute radiation doses larger than 1 Gray (Gy), damage to stem cell progenitors of hematopoietic cells weakens the immune system and leaves the exposed individual susceptible to infection and bleeding. For radiation doses greater than 6 Gy, damage to small intestine epithelial clonogenic cells leads to a reduction in small intestine epithelial lining. Because the epithelial lining provides an essential barrier for defense against bacterial invasion in the bloodstream, damage to epithelial cells can cause diarrhea, bacterial translocation, and sepsis. Due to the recovery time of the different cell systems, these acute radiation sub-syndromes can remain life-threatening for up to 30 days in the case of GI-ARS, and up to 60 days for H-ARS.

Combinations of injuries from radiation, thermal and blast environments cause complex physiological responses that can significantly complicate health risks. Animal studies have quantified the increased effects on the hematopoietic and gastrointestinal systems from combining thermal and blast-related injuries to irradiation (Kiang et al., 2014; Carter et al., 2016; Baker and Valeriote, 1968; Palmer et al., 2011). However, there is minimal human data on combined injuries, making it difficult to develop models that directly predict mortality from combined injury scenarios. As an alternative approach, we have evaluated the literature for biomarkers that we can model and use to predict mortality.

Clinical studies of ICU patients have assessed the prognostic power of various biological measurements as predictive biomarkers of mortality. In Piton et al., 2013, for instance, the amino acid citrulline was determined to be a predictive biomarker of 28-day mortality for critically ill ICU patients. In addition to citrulline, other noteworthy biomarkers of mortality include platelet levels (Vanderschueren et al., 2000; Strauss et al., 2002; Moreau et al., 2007; Marck et al., 2013; Guo et al., 2012; Akca et al., 2002) and the neutrophil-lymphocyte ratio (NLR) (Saliccioli et al., 2015; Akilli et al., 2014; Dilektasli et al., 2016). Biomarkers were evaluated in this study and used to model probability of 30 and 60-day mortality.

## 4 Methods

### 4.1 Small Intestine Damage as a Predictor of 30-Day Mortality

#### 4.1.1 Background

Small intestine damage induced by radiation and burn injuries leads to the death of epithelial cells. Here we present pertinent data used to create our model of small intestine damage as a predictor of 30-day mortality.

There is limited human data on the small intestine response to radiation and burn. However, it has been well-established through animal studies that the primary effect of radiation on the small intestine is the death of proliferating crypt cells (Leshner, 1967; Bond et al., 1965; Potten, 2004). Much less is known about small intestine epithelial response to burn, but rodent studies have revealed that burns induce premature death of villus cells and dampen crypt cell proliferation (Wolf et al., 1999; Carter et al., 2014; Jeschke et al., 2007). We have developed a cell kinetics model (see Figure 4.1) that predicts time-dependent proliferating crypt cell counts, maturing crypt cell counts, and villus cell counts following radiation and burn (Bellman and Stricklin, 2016). Human data was available to parameterize radiation response in this model, while normalized murine data was used to parameterize the burn response (Bellman and Stricklin, 2016). More details of the model are provided in Appendix A.

The amino acid citrulline is produced in enterocytes in the small intestine. Accordingly, plasma citrulline concentration has been correlated with small intestine epithelial cell mass in humans (Guoyao and Morris, 1998; Curis et al., 2005; Crenn et al., 2000; Jianfeng et al., 2005; Luo et al., 2007; Rhoads et al., 2005), and used as a biomarker of bacterial translocation, sepsis and death (Crenn et al., 2014; Wijnands et al., 2015; Su et al., 2015; Piton et al., 2010; Piton et al., 2013; Piton et al., 2011). Specifically, thresholds of 10  $\mu\text{mol/L}$  (Piton et al., 2010) and 12.2  $\mu\text{mol/L}$  (Piton et al., 2013) have been identified as statistically significant predictors of 28-day mortality for ICU patients, compared to a normal citrulline concentration range of 20-50  $\mu\text{mol/L}$  (Pappas et al., 2002).

Low levels of citrulline can be indicative of bacterial translocation, a potentially lethal condition that allows the passage of bacteria from the gastrointestinal tract to various organs (e.g. liver, kidney, spleen) and the bloodstream (Berg, 1999; Vaishnavi, 2013). Bacterial translocation can promote the progression of sepsis, especially in conjunction with a compromised immune system. In order for bacterial translocation to occur, at least one of the following three pathophysiological factors must be present: host immune deficiencies and immunosuppression, disruption of ecologic GI equilibrium, and increased permeability of the intestinal mucosal barrier (Berg, 1999; Vaishnavi, 2013; Magnotti and Deitch, 2005; Deitch, 1990; Gosain and Gamelli, 2005). The model in the present study focuses on increased permeability of the gut mucosal barrier due to a loss of small intestine epithelial cells.

Figure 4.2 provides time-dependent villus cell counts (normalized to pre-insult levels)

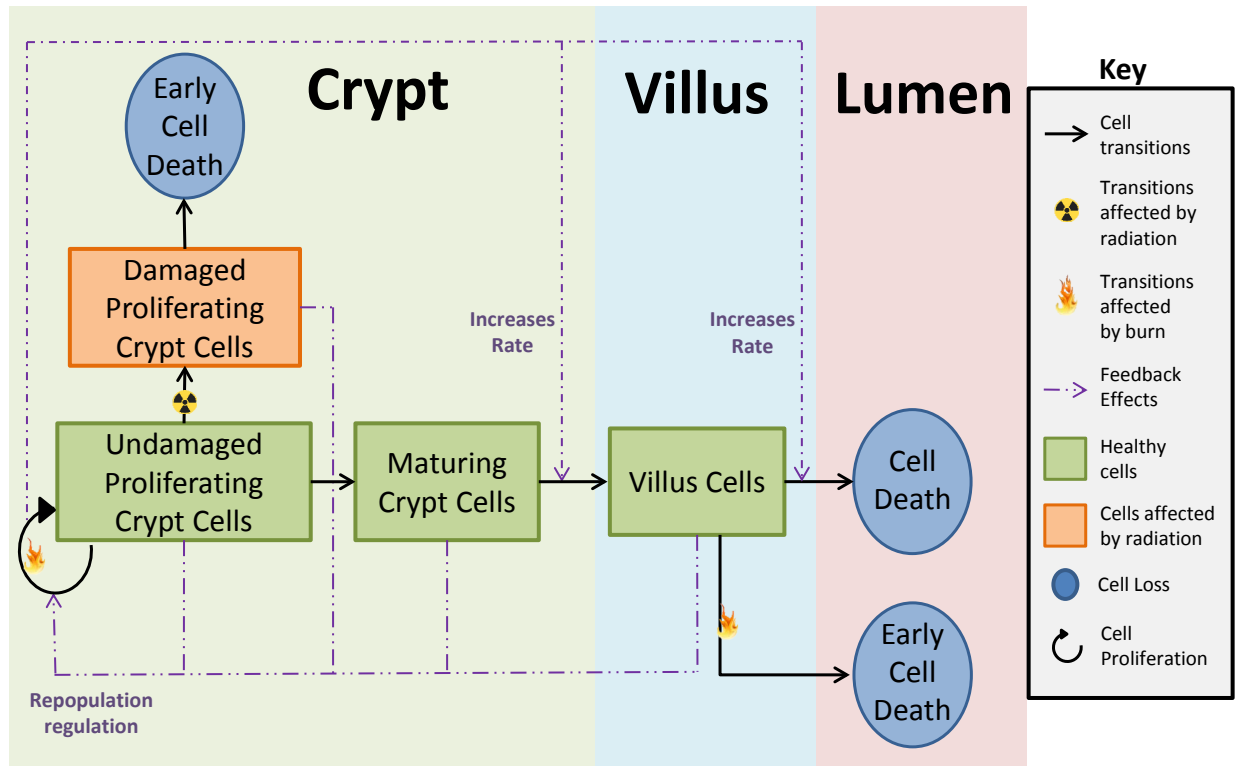


Figure 4.1: Small intestine cell kinetic model.

predicted by the small intestine model in the event of a 10 Gy midline tissue (MLT) radiation dose combined with a 20% total body surface area (TBSA) burn. The figure identifies the villus cell nadir, which can be used to quantify epithelial damage in the small intestine. In this case, an approximate 68% reduction in villus cells is predicted from the combined injury approximately 8 days after exposure.

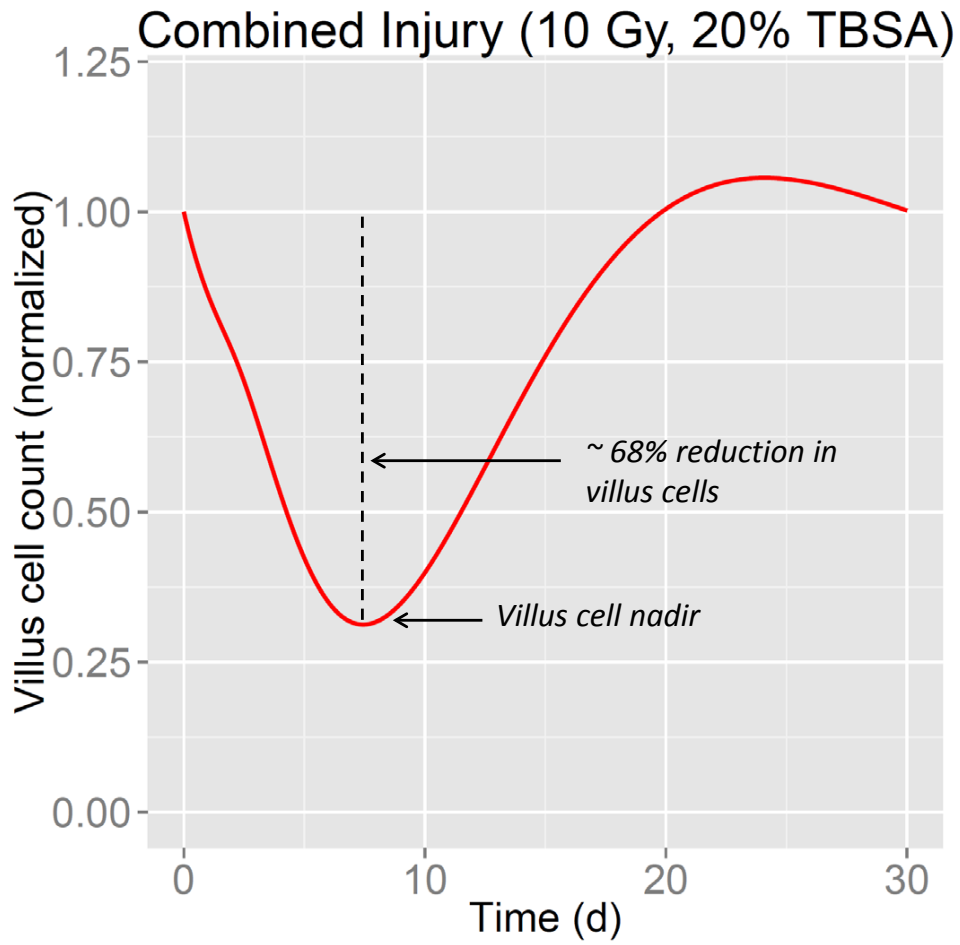


Figure 4.2: Small intestine combined injury example.

### 4.1.2 30-Day Mortality

Data from short bowel syndrome (SBS) individuals and ICU patients were used to develop the SIMM, which predicts 30-day mortality as a function of villus cell reduction (Bellman, 2016). We briefly describe the development of the SIMM in this section.

First, we used ICU data (Piton et al., 2013) to establish a relationship between reduced citrulline levels and the probability of lethality. This relationship was complicated by the fact that some patients in the ICU die of conditions that are not necessarily related to citrulline levels. To account for this unattributable “baseline” level of mortality, we assumed a constant probability of death for these patients, regardless of citrulline levels. We also assumed that the probability of mortality,  $p_C^d$ , is dependent on the multiplicative inverse of the citrulline nadir,  $ci$ , and follows a log-normal cumulative distribution ( $p_C^d(ci) = \int_0^{ci} f_X(t)dt$ , where  $X \sim \ln \mathcal{N}(\mu, \sigma^2)$ ). Optimizing this function against the ICU data, we determined optimal location and scale parameters:  $\mu = -1.83$ , and  $\sigma = 0.42$ . The probability of mortality dependent on the citrulline nadir is presented in Figure 4.3.

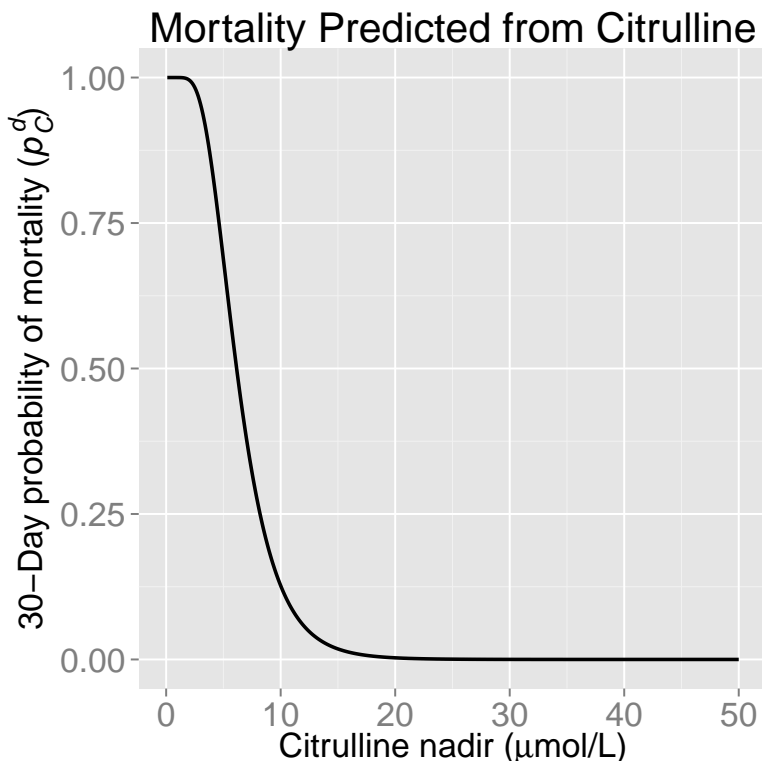


Figure 4.3: 30-Day probability of mortality predicted from citrulline nadir.

SBS data was used to establish a linear relationship between villus cell populations and citrulline concentration (Crenn et al., 2000). It is important to note that an unhealthy gut of an individual exposed to radiation will likely function differently than the gut of a healthy individual with SBS. However, to establish this relationship in our model, we have made the assumption that citrulline loss in these two cases will be directly linked to loss of functional villus cells. We intend to investigate the validity of this assumption in the future.

## 4.2 Platelet Levels as a Predictor of 60-Day Mortality

### 4.2.1 Background

Burn insults result in a drop in circulating platelet levels, which leads to thrombocytopenia, increasing the risk of hemorrhage, hypovolemic shock, sepsis, septic shock and death. The minimum platelet count for burn patients, which is generally reached 3-4 days after ICU admission, has been shown to be predictive of mortality (Vanderschueren et al., 2000; Akca et al., 2002; Moreau et al., 2007; Guo et al., 2012; Marck et al., 2013). Following the drop in platelets, cell count recovery overshoots normal values before a period of prolonged thrombocytosis. This trajectory has consistently been reported in burn patients as well as ICU patients (Marck et al., 2013; Moreau et al., 2007).

Radiation injuries yield a different response for circulating platelets, where prolonged thrombocytopenia causes platelets to slowly reach a minimum about 30 days after exposure before returning to normal levels (Bond et al., 1965; Hempelmann et al., 1952; Howland et al., 1961; Mettler, 2001; Stavem et al., 1985). Mortality predicted from a radiation-induced nadir is not consistent with mortality predicted from a burn-induced nadir, so we decided to only focus on burn in this study. In future studies, we will consider alternative biomarkers, such as the duration of thrombocytopenia, that may be more reliable in predicting mortality from combined radiation and burn injuries.

Our model of thrombopoiesis (Figure 4.4) predicts time-dependent cell counts of mitotic progenitors, megakaryocytes and platelets after burn insults (Wentz et al., 2014a; Wentz et al., 2014b; Wentz et al., 2015a; Wentz et al., 2015b) (Figure 4.4). A sample run of the thrombopoiesis model is provided in Figure 4.5, where circulating platelets respond and recover from a 20% TBSA burn. In this case, an approximate 50% reduction in platelets is predicted at the nadir, about four days following the insult.

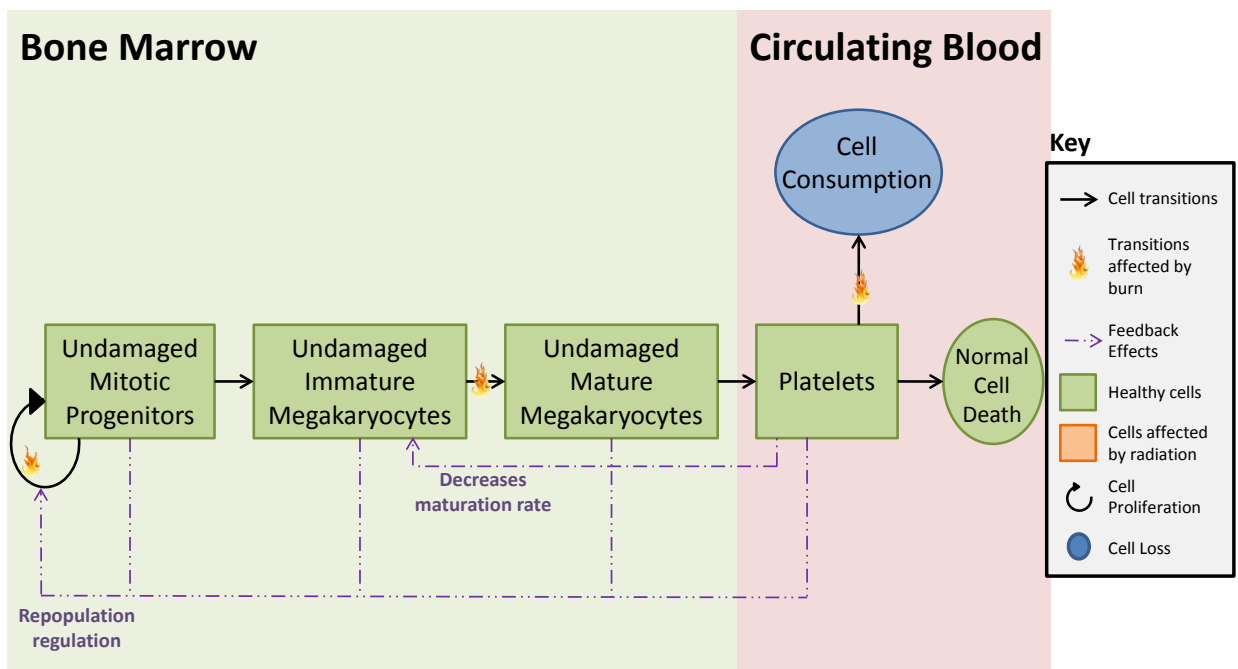


Figure 4.4: Thrombopoiesis cell kinetic model.

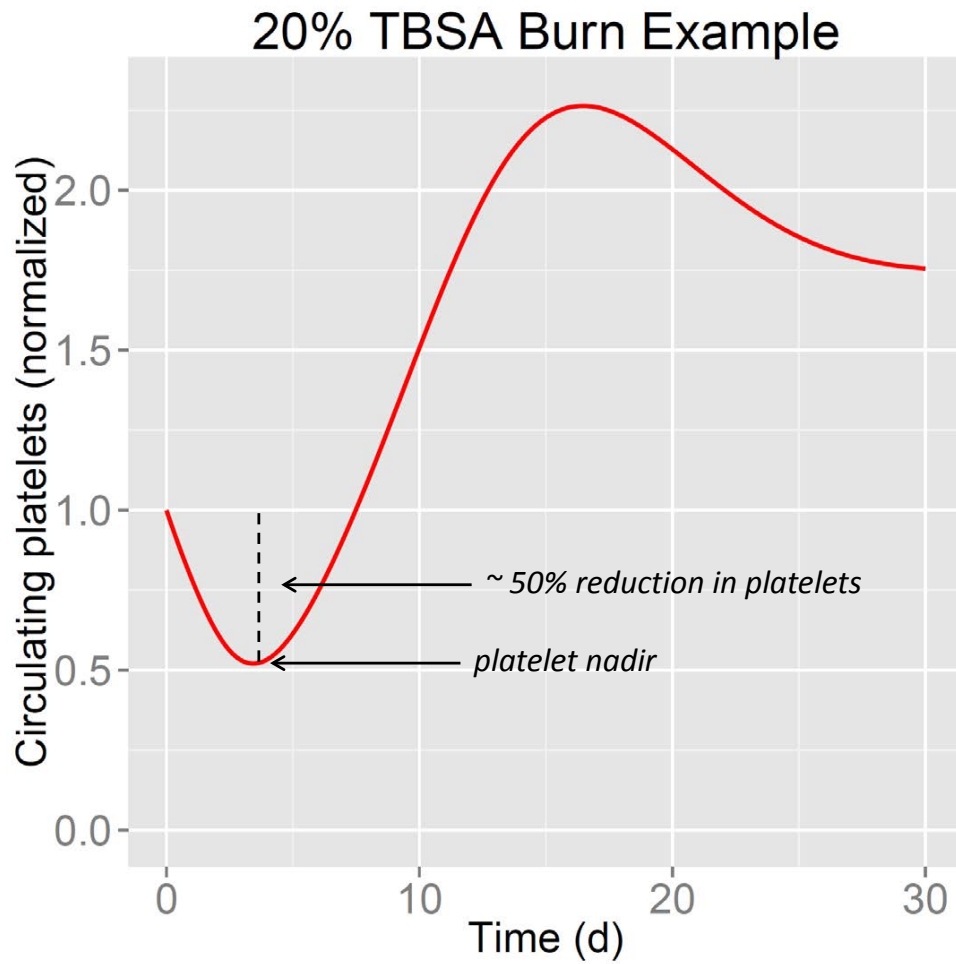


Figure 4.5: Platelet counts of a burn patient.

## 4.2.2 60-Day Mortality

Burn ICU data was used in the development of the PAMM, which predicts the probability of 60-day mortality,  $p_P^d$ , given the percent reduction in platelets at the nadir of the platelet trajectory,  $pr$  (Crary, 2016). Similar to the SIMM,  $p_P^d$  follows a log-normal cumulative distribution ( $p_P^d(pr) = \int_0^{pr} f_X(t)dt$ , where  $X \sim \ln\mathcal{N}(\mu, \sigma^2)$ ), with the following location and scale parameters:  $\mu = 1.83$ , and  $\sigma = 0.43$ .  $p_P^d$  is provided in Figure 4.6. Due to data limitations (see Crary, 2016 for details), and the fact that patients can survive after losing over 80% of their platelets (Guo et al., 2012), the fit of this data does not exceed a probability of mortality of 0.66. The impact of this limitation is discussed in more detail in Section 6 with respect to the domain of applicability of the model.

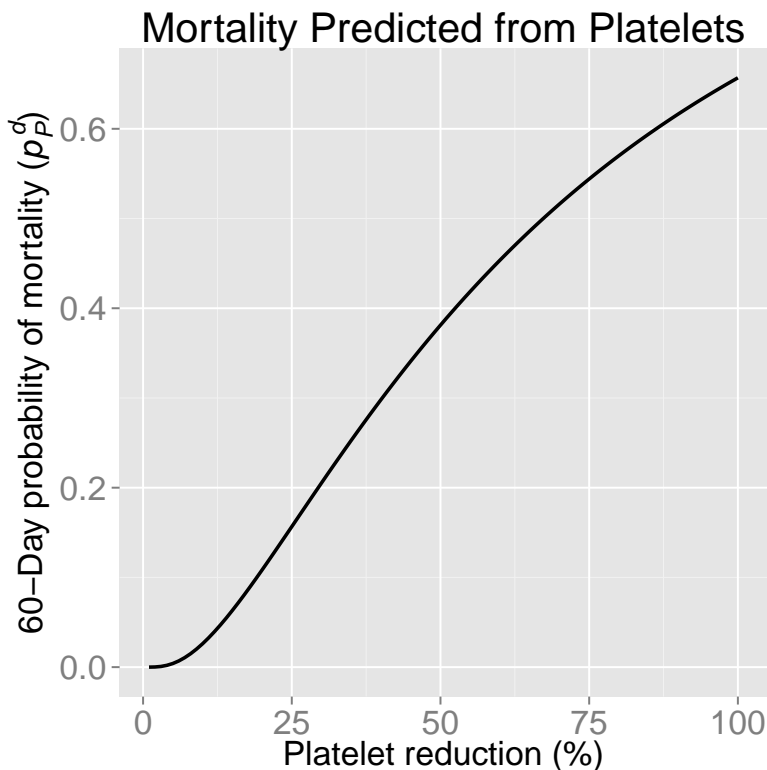


Figure 4.6: 60-Day probability of mortality predicted from platelet nadir.

## 4.3 Neutrophil to Lymphocyte Ratio

### 4.3.1 Background

Tissue damage from injury induces a localized inflammatory response involving components of the innate and adaptive immune systems. Soon after injury, the inflammatory response results in changes in the local vasculature that lead to vasodilation, increased vascular permeability, and increased blood flow (Serhan et al., 2010). These changes contribute to the recruitment of leukocytes (white blood cells), plasma proteins, and fluids into the damaged tissue (Ashley et al., 2012). Normally, the perturbations in neutrophil and lymphocyte levels that occur following injury rapidly return to normal. Resolution of inflammation occurs by leucocyte removal by apoptosis or the lymphatic system (Serhan et al., 2010).

Severe traumatic injury accompanied by infection or additional tissue damage can lead to a persistent state of inflammatory dysregulation characterized by an overactivation of the innate immune response (primarily neutrophils) followed by a strong anti-inflammatory response that causes suppression of adaptive immunity resulting in decreased T cell function (Valparaiso et al., 2015). Neutrophils release reactive oxygen species (ROS) and proteases to fight pathogens and remove damaged tissue. Even a properly functioning inflammatory response causes some damage to tissue of the host organism (Medzhitov, 2008). When inflammation does not resolve normally, the tissue damage caused by the neutrophil response is injurious and can result in a positive feedback loop that exacerbates the inflammatory response. Lymphocytes are an important component of the adaptive immune response (Barrett et al., 2009) and are crucial for the host response to infection. Reduced lymphocyte levels impair the ability of the host to respond to infection that inevitably accompanies serious traumatic injury. The schematic shown in Figure 4.7 illustrates how tissue injury coupled with physiological and immunologic disturbances interact to contribute to post-injury morbidity and mortality (Valparaiso et al., 2015).

Disorders that stem from dysregulated inflammation include acute respiratory distress syndrome (ARDS), sepsis, and multiple organ dysfunction syndrome (MODS). These disorders are commonly seen in patients in ICUs. In particular, most ICU patients have some degree of organ dysfunction and as many as 50% have MODS. Mortality from MODS varies depending on the number of organ systems affected, with mortality associated with three or more organ system failures ranging from 20-100% (*Irwin and Rippe's Intensive Care Medicine* 2011). MODS is the most common reason for long stays in the ICU. Given the serious risks associated with inflammation-related disorders resulting from traumatic injuries, it is crucial that the patients most at risk are identified early so interventions and treatments can be appropriately prioritized. The cellular and molecular events that occur during inflammation are similar whether injury occurs through blunt, penetrating, or burn initiating mechanisms; therefore, it is possible to find biomarkers useful for identifying patients at risk of developing disorders of dysregulated inflammation.

A high-level schematic of the body's response to traumatic injury is shown in Figure 4.8 (Lord et al., 2014). Signals produced by stressed, damaged, or malfunctioning tissues act as endogenous inducers of inflammation (Medzhitov, 2008, Kotas and Medzhitov, 2015). The host senses pathogens by both a direct mechanism, where host proteins bind microbial products, and an indirect mechanism, using host molecules that detect products of host

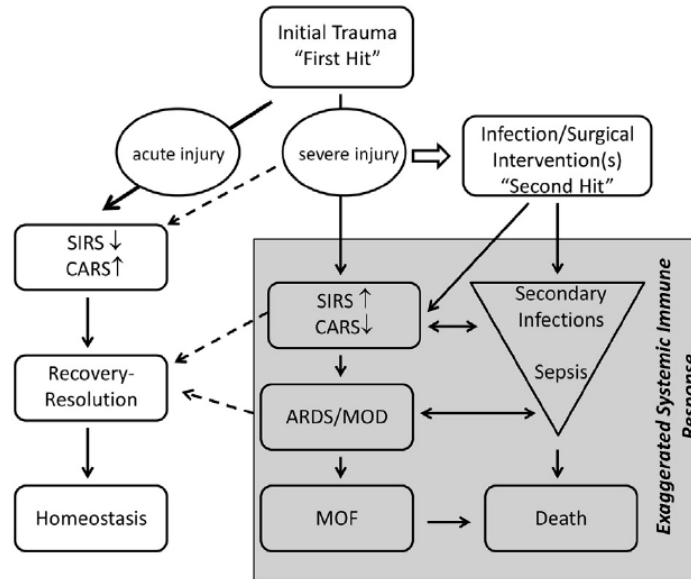


Figure 4.7: Interactions of tissue injury with physiological and immunological disturbances that lead to post-injury morbidity and mortality (Valparaiso et al., 2015).

cell necrosis (Nathan and Ding, 2010). The host uses necrosis of its own cells as one of the immune system’s earliest and best-amplified signals to report the dissemination of a possible infection. Damage-associated molecular patterns (DAMPs) are released by injured and necrotic cells in damaged tissue and secreted by neutrophils that have been recruited to the site of injury. DAMPs are potent activators of several types of immune cell, including immune cells that are involved in the complement response. Activation of these cell types triggers the release of numerous inflammatory mediators like cytokines and interleukins. Peptides and DNA released from the mitochondria of damaged cells elicit a particularly potent response, most likely due to the mitochondria of eukaryotes having evolved from an aerobic bacterium living within an archaeal host cell (see the endosymbiotic theory Margulis and Bermudes, 1985). Infection of some degree nearly always accompanies traumatic injury. Damage to the skin or gastrointestinal tract can lead to exposure to exogenous or endogenous pathogens which causes further stress to the patient. Analogous to the DAMPs released or secreted by endogenous cells, infection results in exposure to a number of non-self pathogen-associated molecular patterns (PAMPs) that also activate the immune system (Lord et al., 2014).

### 4.3.2 NLR Studies

The physiological inflammatory and immune response to various stressful events, including traumatic injury, is characterized by changes in the levels of certain circulating leukocytes (white blood cells) (de Jager et al., 2010). Neutrophil counts typically increase and lymphocyte counts decrease. The neutrophil to lymphocyte ratio (NLR), has been recognized as a biomarker of a patient’s level of inflammation and stress (Zahorec, 2001), and an elevated NLR identifies patients that have less physiological reserve to survive the inflammatory insult resulting from a traumatic injury (Saliccioli et al., 2015). The NLR has demonstrated

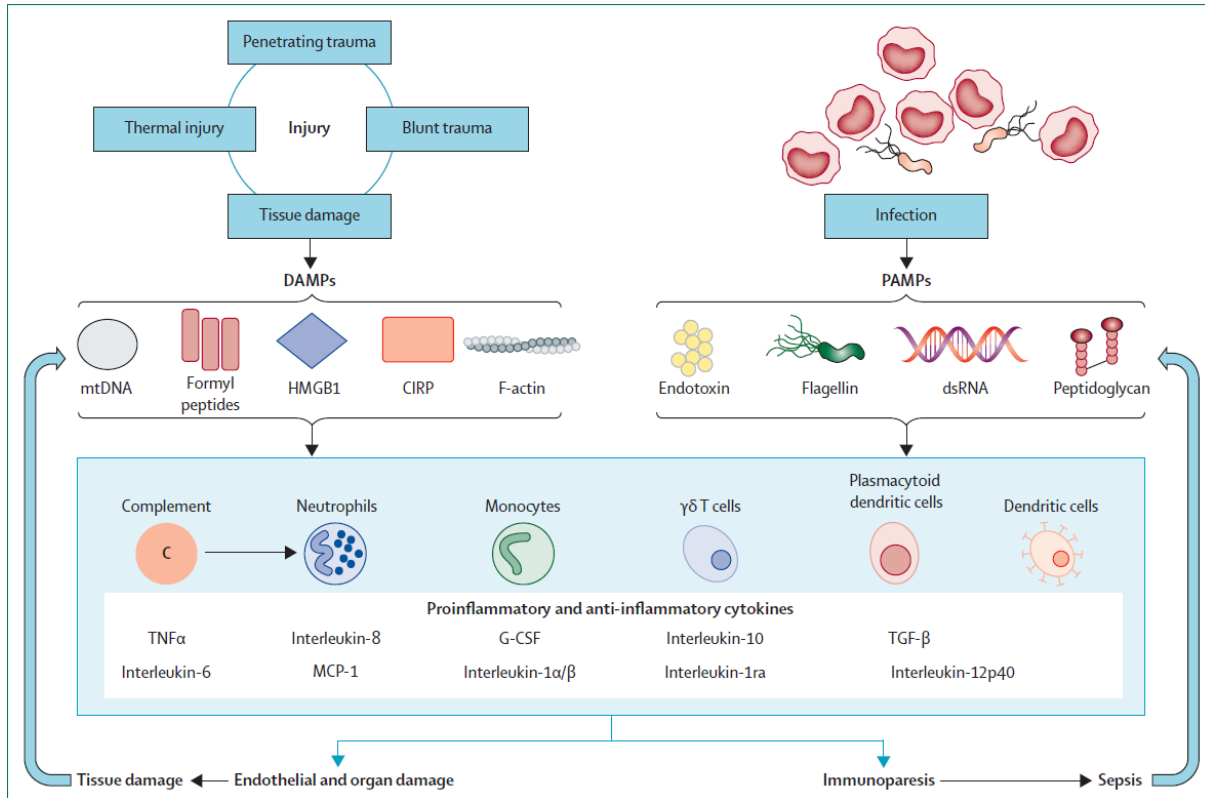


Figure 4.8: Activation of the inflammatory response in response to trauma, tissue damage, and infection (Lord et al., 2014).

prognostic value with trauma patients (Akilli et al., 2014, Dilektasli et al., 2016, Salciccioli et al., 2015), but has also been useful clinically with patients experiencing different types of cancer (Absenger et al., 2013, Rimando et al., 2016, Salman et al., 2016), sepsis (Riché et al., 2015, Salciccioli et al., 2015, Liu et al., 2016), radiation poisoning (Hérodin et al., 2012, Blakely et al., 2014, Ossetrova et al., 2014, Valente et al., 2015), mushroom poisoning (Koylu et al., 2014), and suicide risk in patients with bipolar disorder (Ivković et al., 2016). The NLR is easily obtained using standard clinical measures, and is a fast and efficient means for identifying patients at high risk of potentially deadly complications. The prognostic value of the NLR is a consequence of the centrality and function of these cell types in the inflammatory response.

The NLR has been used as an indicator for a large number of disease groups. Unfortunately, no manuscripts could be found associating NLR with mortality due solely to burns or radiation exposure, the diseases most relevant for use with HENRE. Although, the NLR has been reported as a biomarker of radiation exposure (*The medical aspects of radiation incidents* 2013), detailed information on the derivation of cutoff values was not provided. Three manuscripts were found that discuss the prognostic value of the NLR in critically ill (Akilli et al., 2014, Salciccioli et al., 2015) or trauma patients (Dilektasli et al., 2016). There are no patients with burn or radiation injuries in these studies; however, the generality of the inflammatory response makes the reasonable assumption that the levels of the NLR associated with mortality will be relevant for different disease groups. This claim is supported

by recent work that found very high correlations among the human transcriptional responses of inflammation-related genes in response to trauma, burns, and endotoxemia (Seok et al., 2013).

The study by Akilli et al., 2014 was a prospective, observational cohort study that followed 373 critically ill patients that were admitted to the emergency department at a single medical center between January 1, 2013 and August 10, 2013. All patients in the study required treatment administered in the ICU. The median age of the patients was 74, and 54.4% were male. The primary endpoints were in-hospital mortality and 6-month mortality. Figure 4.9 shows the receiver operating characteristic (ROC) curve used to find the optimal NLR cutoff for distinguishing between patients that survived and patients that died. ROC analysis is a common technique used to evaluate the predictive power of a biomarker by plotting the true positive rate against the false positive rate, where the biomarker is considered to have significant power if area under the curve (AUC) is much larger than 0.5 (with a maximum of 1). In this case, the optimal NLR cutoff was found by Youden's method (Youden, 1950) to be 11.9. The AUC of the ROC curve is relatively modest at 0.61, indicating that the NLR only weakly discriminates between surviving and non-surviving patients in this study. Kaplan-Meier curves of patients grouped by NLR quartile are shown in Figure 4.10. Survival decreases with increasing NLR quartile.

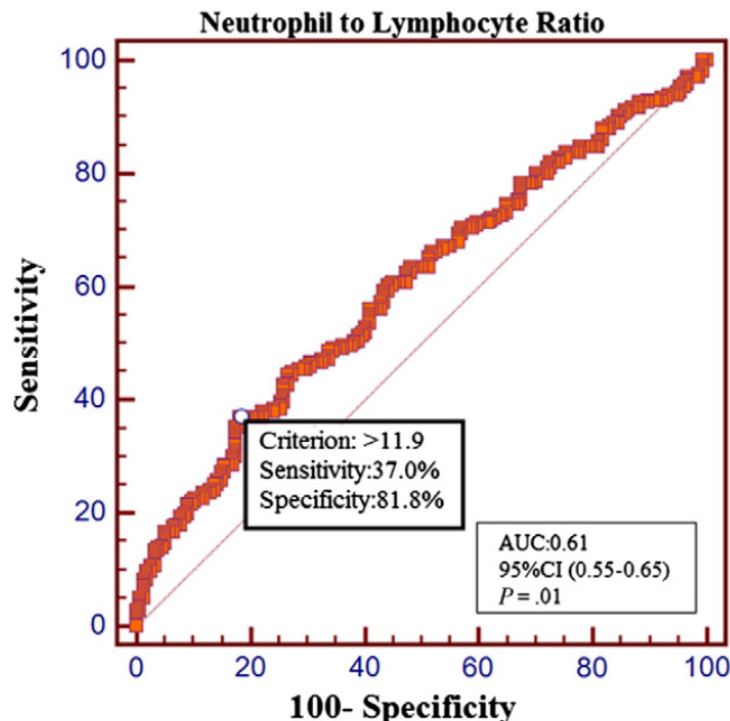


Figure 4.9: Receiver operating characteristic curve of NLR to predict mortality (Akilli et al., 2014).

Saliccioli et al., 2015 also performed an observational cohort study on ICU patients. The study used data collected from the Multiparameter Intelligent Monitoring in Intensive Care (MIMIC II) clinical database Saeed et al., 2011. There were a total of 5,056 patients

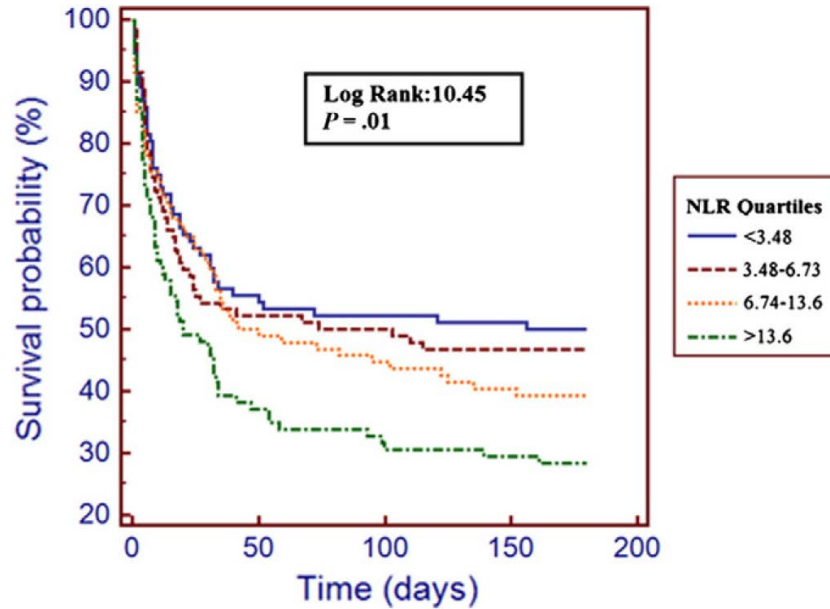


Figure 4.10: Kaplan-Meier survival curves for NLR quartiles determined in Akilli et al., 2014.

that were over 17 years old, had complete neutrophil and lymphocyte data at admission, and had full sets of covariates. The median age was 65 (interquartile range of 51-78), and 53% of the patients were male. The primary endpoint of the study was 28-day mortality, secondary endpoints were in-hospital mortality and 1-year mortality. Subjects were grouped by NLR quartile, with cutpoints at 4.99, 8.90, and 16.21. There was a statistically significant relationship between increasing quartile of NLR quartile and 28-day mortality in an unadjusted analysis over time. The relationship remained significant after adjusting with covariates. All secondary outcomes showed similar trends in mortality. The relationship between NLR quartile and mortality is also illustrated by Figure 4.11 using the data from the study by Saliccioli et al., 2015.

The Dilektasli et al., 2016 study is a retrospective cohort study consisting of 1,007 trauma patients 16 years or older admitted to the surgical intensive care unit of the LAC + USC Medical Center between January 2013 and January 2014. The median age was 49 and 74% were male. The performance of the classifiers from the Dilektasli et al., 2016 manuscript can be seen in Figure 4.12, which shows the ROC curves obtained for NLR values measured on hospital days 2 and 5. Optimal cutoff values distinguishing patients that died and survived in the first 10 days of hospitalization were determined using the Youden index and found to be 8.19 for hospital day 2 and 7.92 for hospital day 5. A higher NLR, measured at 2 or 5 days, was significantly associated with higher in-hospital mortality and with reduced overall survival. Kaplan Meier curves of the overall survival where patients were stratified using the cutoff values determined by the ROC analysis are shown in Figure 4.13.

The median ages of the study populations in the Akilli et al., 2014 and Saliccioli et al., 2015 studies are high. Many of the patients in these study populations are likely suffering from complicated geriatric syndromes or complications related to chronic diseases. The sample size of the Akilli et al., 2014 study is also relatively small. The population studied

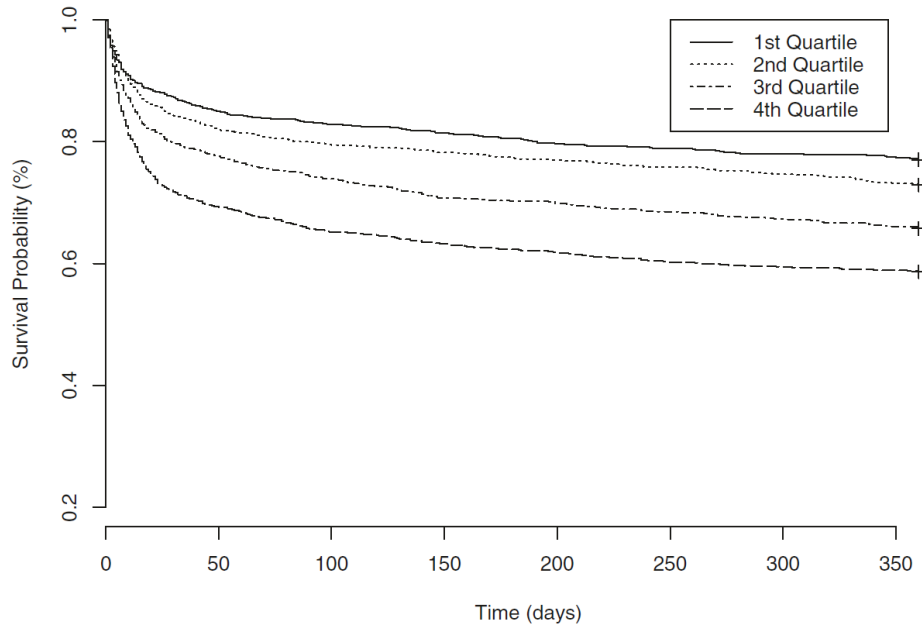


Figure 4.11: Kaplan-Meier survival curves for 1-year mortality based on NLR quartiles determined in Saliccioli et al., 2015. Quartile cutpoints were NLR values of 4.99, 8.90, and 16.21. Patients in the fourth NLR quartile (NLR > 16.21) had the lowest survival probability at one year.

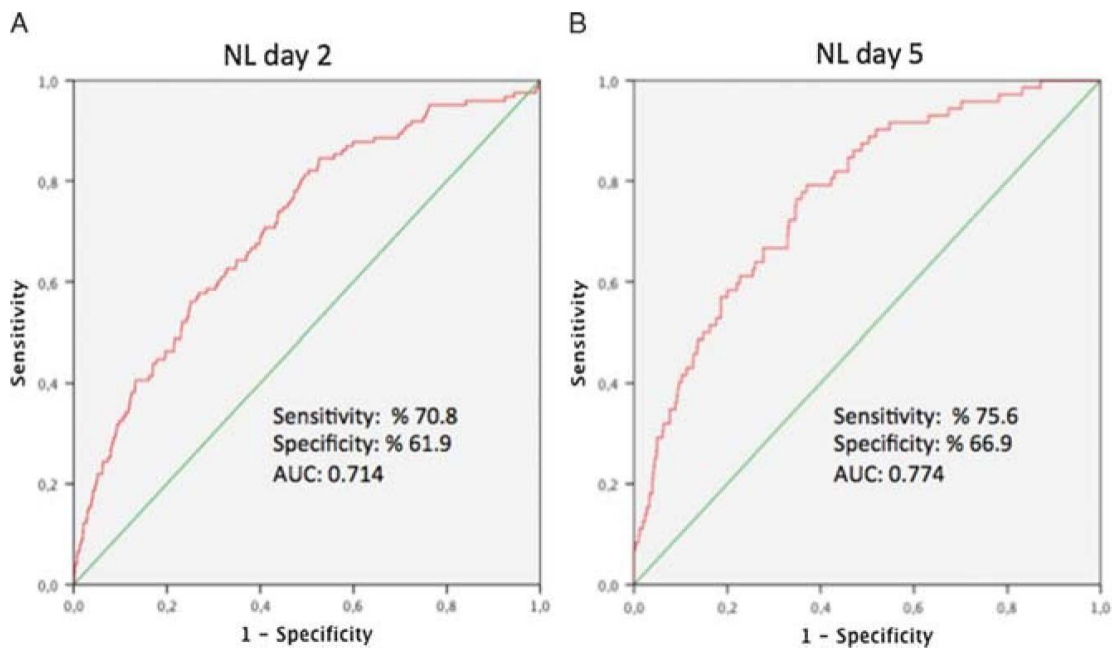


Figure 4.12: ROC curves for (A) the NLR on hospital day 2 and (B) hospital day 5 (Dilektasli et al., 2016).

in Dilektasli et al., 2016 consists primarily of patients admitted to the ICU for blunt or penetrating injuries. The median age of the study population is considerably lower than

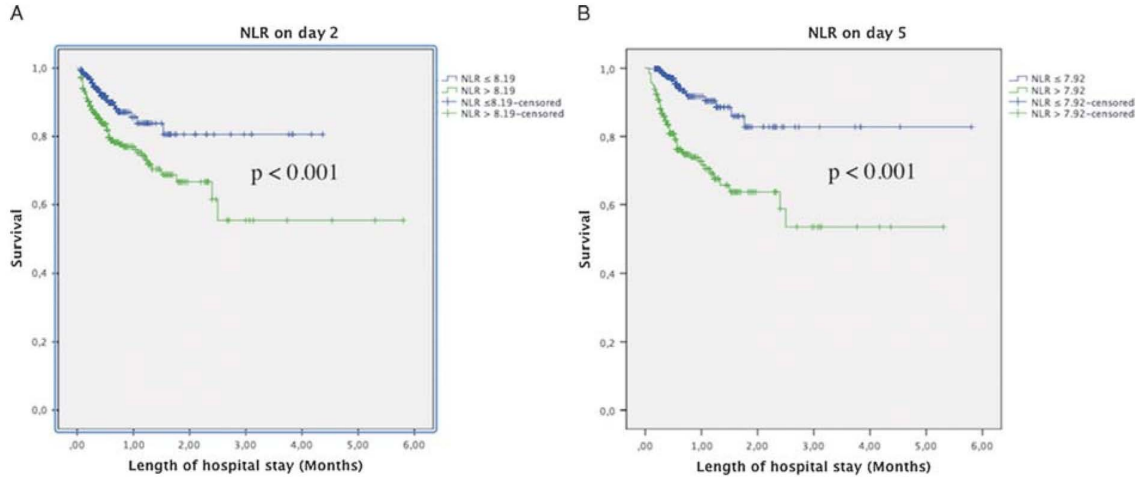


Figure 4.13: Kaplan Meier survival curves for (A) the day 2 cutoff of 8.19 and (B) the day 2 cutoff of 7.92 (Dilektasli et al., 2016).

those of the Akilli et al., 2014 and Salciccioli et al., 2015 populations.

HENRE contains models that describe the dynamics of lymphocyte and granulocyte populations in response to burn or radiation injury (Wentz et al., 2014a, Wentz et al., 2015a). Currently, these models represent part of the complex biology associated with inflammation; for example, they do not simulate the processes associated with dysregulated inflammation that would be expected to be seen on the pathway to ARDS, sepsis, and MODS. A quantitative model relating the NLR to mortality would not be useful at this time given the limited biological domain of the existing models and state of the available data. However, this section demonstrates the centrality of the inflammatory process in the combined-injury scenario and suggests directions for further development of the capabilities of HENRE.

## 5 Results

GI-ARS is expected to play a large role in 30-day mortality, and our model allows us to quantify the added risk of mortality from burns for ARS casualties. Figure 5.1 presents predictions of 30-day mortality from various radiation and burn combined injuries (CIs) calculated from the SIMM. These simulations are presented as radiation dose response curves at fixed burn insults.

Assuming no burn (0% TBSA), the model predicts an LD50/30 (the lethal dose for 50% of the population by day 30) of approximately 12.5 Gy (MLT). This is a very large radiation dose, but it lies in an expected range when compared to lethal doses for other scenarios. For example, the human LD50/60 assuming no treatment is estimated to be 4.1 Gy (FIA) (Anno et al., 2003), which is approximately 2.9 MLT. Furthermore, the LD50/48hr (the lethal dose for 50% of the population by 48 hours) assuming no treatment has been estimated to be 31 Gy (FIA) (Millage and Crary, 2016), which is approximately 22.1 Gy (MLT). Therefore, we would expect the LD50/30, assuming no treatment, to fall between 2.9 and 22.1 Gy (MLT). Assuming standard care, the lethal dose at a specific time will increase; therefore, the value of 12.5 Gy (MLT) for the LD50/30 does not seem unreasonable.

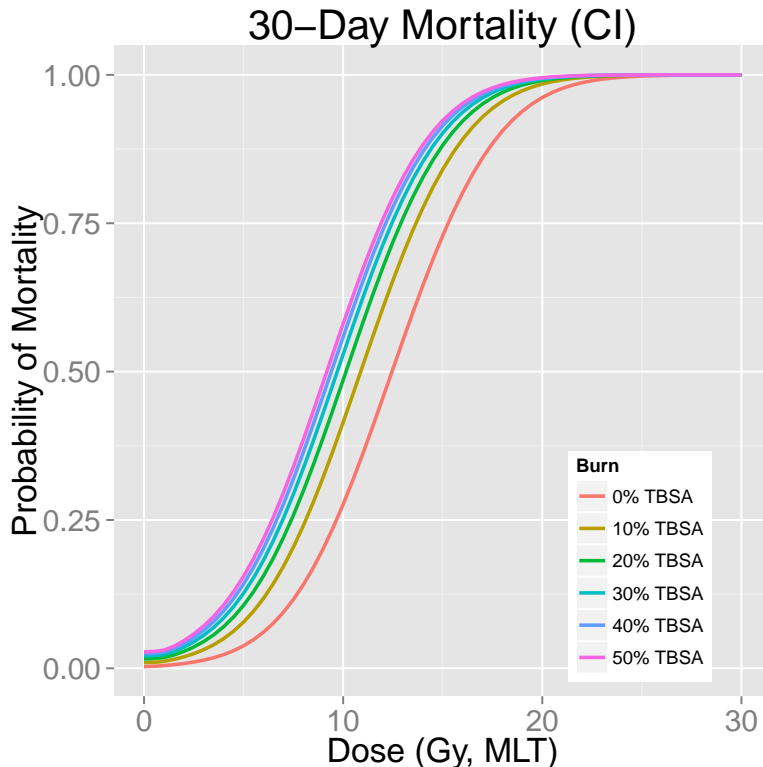


Figure 5.1: Probability of 30-day mortality predicted by the SIMM.

These results suggest that the contribution of burn (measured by % TBSA) to GI-ARS-related mortality is relatively minor. This can be attributed to the fact that the SIMM

only accounts for death from bacterial translocation through the breakdown of the small intestine epithelial lining. Because the small intestine model was initially developed with the intention of modeling ARS, the SIMM does not account for mortality from risks such as wound infections associated with burns. Although bacterial translocation is a primary contributing factor to death for GI-ARS, infection through burn wounds is particularly lethal when burns exceed 40% TBSA (Gang et al., 1999; Taneja et al., 2004). For this reason, we assume the model is appropriate for low to medium burn sizes.

Results from the PAMM are provided in Figure 5.2. The LA50/60 (the percentage of the body surface area burned in which 50% mortality results by day 60) from this model is approximately 37%, which is slightly lower than the LA50/60 of 45% predicted by our 60-day mortality model assuming no treatment (Stricklin, 2013b). Although we would expect to see a higher LA50/60 here, it is encouraging to see that these numbers are fairly similar. We intend to revisit this inconsistency in future studies.

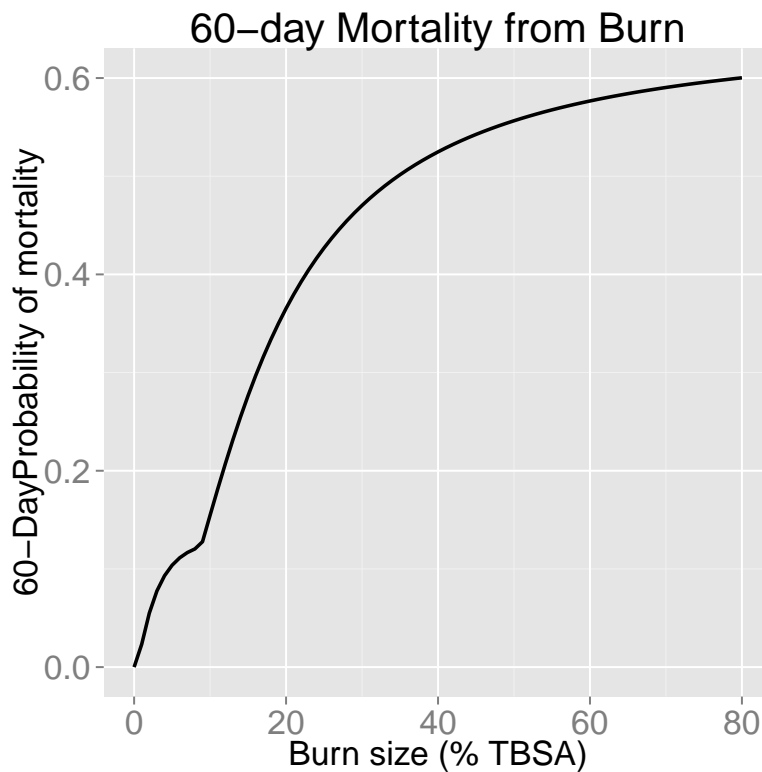


Figure 5.2: Probability of 60-day mortality predicted from platelet reduction.

Together, the SIMM and PAMM provide new capabilities for the 30 and 60-day mortality models currently in HENRE. The SIMM is a first step in developing combined injury capabilities of the 30-day mortality model, and the PAMM is a first step in predicting 60-day mortality with treatment.

## 6 Discussion

The purpose of this study was to develop models that predict the probability of death of an individual through the use of predictive biomarkers. We used relevant hospital patient data to correlate biomarker levels with the probability of 30 and 60-day mortality. Models that represent cell kinetics were used to predict biomarker levels, which in turn were used to predict mortality.

The SIMM and PAMM continue to build capabilities in HENRE to predict mortality due to combined injury. These models consider the health outcomes for individuals receiving standard care, and represent significant steps in capturing critical physiological processes and systems affected by radiation and burn. The majority of the models previously developed for this effort assume that no treatment is available. Previously the only model in HENRE capable of taking treatment into account was the 60-day mortality model. For this effort, we have added standard care to the models of 60-day mortality from burns and 30-day mortality from radiation and burns (see Figure 1.1).

As with all models, there are limitations to the SIMM and PAMM, most notably, with respect to the domain of applicability suggested by the underlying data. The SIMM, for example, predicts the probability of mortality due to GI-ARS for combined radiation and burn injury. However, we recognize that the model development was driven primarily by studies on radiation effects. Burn complicates the physiological response considerably in ways that are not currently well represented in the literature, particularly at lower radiation levels. Consequently, we believe that the domain of applicability for the SIMM is limited to radiation and burn environments as depicted in Figure 6.1 A. That is, the reliability of the model predictions is considered to be higher for environments in which the radiation exposure is relatively high, and the % TBSA is relatively low.

For the PAMM, we noted earlier that the maximum probability of mortality is 66%, even at 100% platelet loss. As with the SIMM, the PAMM is not considered reliable for significant burns (e.g., in excess of 60% TBSA) because it does not adequately capture the physiological response and elevated risk for burns of this magnitude. However, we do not anticipate this limitation to have a large impact on casualty estimations for all scenarios. For instance, at Hiroshima and Nagasaki, over 90% of burns were flash burns, which rarely cover more than 50% TBSA (Oughterson and Warren, 1956). The domain of applicability for the PAMM is represented by Figure 6.1 B.

Lastly, the research that we conducted on the NLR underscored the need for discussion regarding the utility of developing response-specific models that are not fully integrated with other mechanistic models in HENRE. Although the research on NLR is promising, the benefit of adding an NLR model based on currently available data was considered to be negligible. However, implicit in the discussion of inflammatory response physiology in Section 4.3, is the need to consider “next generation” capabilities for HENRE, namely, the full integration of response-specific models within a framework that includes inflammation at its core. Ultimately, the fidelity of HENRE’s predictions on injury severity and the time course of disease will depend on the ability of the model to integrate exposure and effect through time for alternative treatment scenarios. The NLR discussion provides an

excellent basis for “next gen” discussions that will shape the future development of HENRE capabilities.

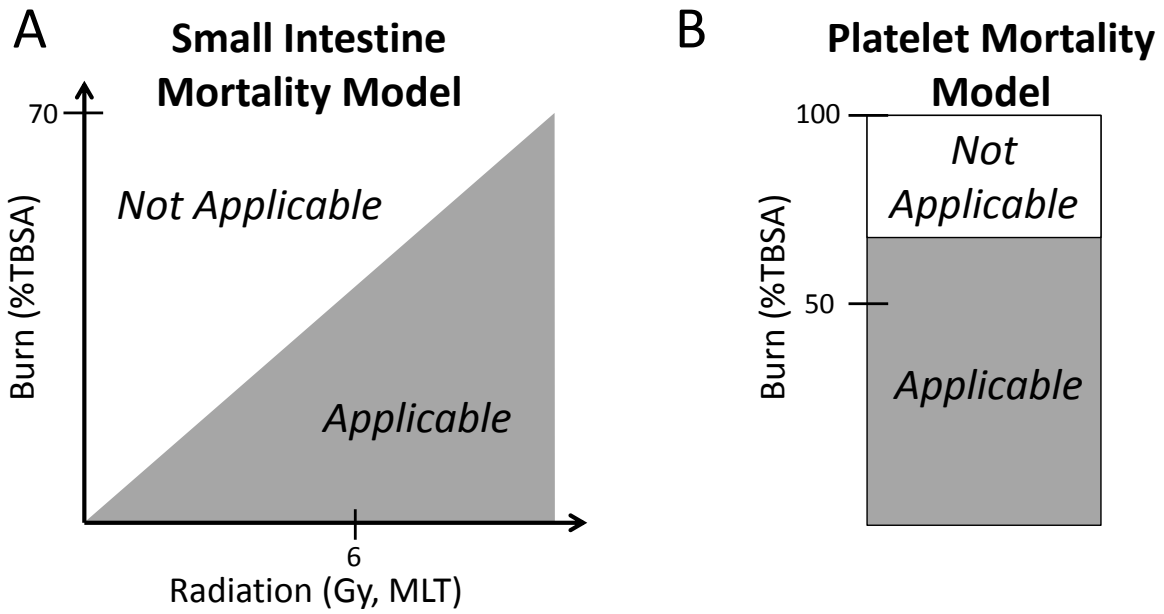


Figure 6.1: Domain of applicability for the small intestine and platelet mortality models.

## 7 Future Work

We continuously aim to improve each of the components of HENRE. The models in this study were developed to expand the domain of applicability of the 30 and 60-day mortality models in HENRE by accounting for treatment of individuals exposed to IND environments. We recognize that there are limitations for these models, and we aim to address these in future studies. This can be accomplished by collecting more data to train and validate our models, as well as performing sensitivity and uncertainty analysis to test the reliability of the models.

In order to continue to improve the capability of the mortality models in HENRE, we also aim to expand the context with which our mortality models are defined. For instance, the mortality models only account for demographics (age and gender) in the context of 60-day radiation-induced mortality. In the future, we would like to account for demographics in the 30-day and 48-hour models. We would also like to account for demographic modifications in the context of combined injury. In addition, we would like to assess the use of the NLR to predict mortality with the granulocyte and lymphocyte cell kinetic models built into HENRE.

## References

- Absenger, G et al. (2013). “Preoperative neutrophil-to-lymphocyte ratio predicts clinical outcome in patients with stage II and III colon cancer.” In: *Anticancer Res* 33.10, pp. 4591–4594.
- Akca, S et al. (2002). “Time course of platelet counts in critically ill patients”. In: *Critical care medicine* 30.4, pp. 753–756.
- Akilli, NB et al. (2014). “Prognostic importance of neutrophil-lymphocyte ratio in critically ill patients: short- and long-term outcomes.” In: *Am J Emerg Med* 32.12, pp. 1476–1480.
- Anno, G. H. et al. (2003). “Dose response relationships for acute ionizing-radiation lethality”. In: *Health Physics* 84.5, pp. 565–575.
- Ashley, NT, ZM Weil, and RJ Nelson (2012). “Inflammation: Mechanisms, costs, and natural variation”. In: *Annu. Rev. Ecol. Evol. Syst.* 43.1, pp. 385–406.
- Baker, DG and FA Valeriote (1968). “The effect of x-irradiation and thermal burn on the intestinal mucosa”. In: *Canadian journal of physiology and pharmacology* 46.3, pp. 533–536.
- Barrett, KE et al. (2009). *Ganong’s review of medical physiology (enhanced EB)*. McGraw-Hill Education.
- Bellman, J (2016). *Small intestine villus count decline as a prognostic indicator of 30-day mortality*. Tech. rep. ARA/HS-TN-16-014. Applied Research Associates, Inc.
- Bellman, J and D Stricklin (2016). *A mathematical model of the human small intestine following acute radiation and burn exposures*. Tech. rep. DTRA-TR-16-059.
- Berg, R (1999). “Bacterial translocation from the gastrointestinal tract”. In: *Advances in Experimental Medicine and Biology* 473, pp. 11–30.
- Blakely, WF et al. (2014). “Further biodosimetry investigations using murine partial-body irradiation model.” In: *Radiat Prot Dosimetry* 159.1-4, pp. 46–51.
- Bond, V, T Fliedner, and J Archambeau (1965). *Mammalian radiation lethality*. Academic.
- Carter, SR et al. (2016). “Neutrophil accumulation in the small intestine contributes to local tissue destruction following combined radiation and burn injury:” in: *Journal of Burn Care & Research* 37.2, pp. 97–105.
- Carter, Stewart R. et al. (2014). “Neutrophil Accumulation in the Small Intestine Contributes to Local Tissue Destruction Following Combined Radiation and Burn Injury”. In: *Journal of Burn Care & Research* 37.2, pp. 97–105.
- Crary, D (2016). *Platelet count decline as a prognostic indicator of lethality in ICU and burn patients*. Tech. rep. ARA/HS-TN-16-012.
- Crenn, P et al. (2000). “Postabsorptive plasma citrulline concentration is a marker of absorptive enterocyte mass and intestinal failure in humans”. In: *Gastroenterology* 119.6, pp. 1496–1505.
- Crenn, P et al. (2014). “Plasma l-citrulline concentrations and its relationship with inflammation at the onset of septic shock: A pilot study”. In: *Journal of Critical Care* 29.2, 315.e1–315.e6.
- Curis, E et al. (2005). “Almost all about citrulline in mammals”. In: *Amino Acids* 29.3, pp. 177–205.

- de Jager, CPC et al. (2010). "Lymphocytopenia and neutrophil-lymphocyte count ratio predict bacteremia better than conventional infection markers in an emergency care unit." In: *Crit Care* 14.5, R192.
- Deitch, E (1990). "Bacterial translocation of the gut flora". In: *The Journal of Trauma* 30, S184–189.
- Dilektasli, E et al. (2016). "The prognostic value of neutrophil to lymphocyte ratio on mortality in critically ill trauma patients." In: *J Trauma Acute Care Surg*.
- Gang, R et al. (1999). "Pseudomonas aeruginosa septicemia in burns". In: *Burns* 25.7, pp. 611–616.
- Gosain, A and R Gamelli (2005). "Role of the gastrointestinal tract in burn sepsis". In: *The Journal of Burn Care & Rehabilitation* 26.1, pp. 85–91.
- Guo, F et al. (2012). "Association of platelet counts decline and mortality in severely burnt patients". In: *Journal of Critical Care* 27.5, 529.e1–529.e7.
- Guoyao, WU and SM Morris (1998). "Arginine metabolism: nitric oxide and beyond". In: *Biochemical Journal* 336.1, pp. 1–17.
- Hempelmann, LH, H Lisco, and JG Hoffman (1952). "The acute radiation syndrome: a study of nine cases and a review of the problem". In: *Annals of Internal Medicine* 36.2:1, pp. 279–510.
- Hérodin, F et al. (2012). "Assessment of total- and partial-body irradiation in a baboon model: preliminary results of a kinetic study including clinical, physical, and biological parameters." In: *Health Phys* 103.2, pp. 143–149.
- Howland, JW et al. (1961). *Diagnosis and treatment of acute radiation injury: proceedings of a scientific meeting jointly sponsored by the IAEA and the WHO, Geneva, 17-21 Oct 1960*. Columbia University Press, New York, pp. 11–26.
- Irwin and Rippe's Intensive Care Medicine* (2011). Lippincott Williams & Wilki.
- Ivković, M et al. (2016). "Neutrophil-to-lymphocyte ratio predicting suicide risk in euthymic patients with bipolar disorder: Moderatory effect of family history." In: *Compr Psychiatry* 66, pp. 87–95.
- Jeschke, MG et al. (2007). "Gut Mucosal Homeostasis and Cellular Mediators after Severe Thermal Trauma and the Effect of Insulin-Like Growth Factor-I in Combination with Insulin-Like Growth Factor Binding Protein-3". In: *Endocrinology* 148.1, pp. 354–362.
- Jianfeng, G et al. (2005). "Serum citrulline is a simple quantitative marker for small intestinal enterocytes mass and absorption function in short bowel patients". In: *Journal of Surgical Research* 127.2, pp. 177–182.
- Kiang, JG et al. (2014). "Ghrelin therapy improves survival after whole-body ionizing irradiation or combined with burn or wound: amelioration of leukocytopenia, thrombocytopenia, splenomegaly, and bone marrow injury". In: *Oxidative Medicine and Cellular Longevity* 2014, pp. 1–12.
- Kotas, ME and R Medzhitov (2015). "Homeostasis, inflammation, and disease susceptibility." In: *Cell* 160 (5), pp. 816–827.
- Koylu, R et al. (2014). "Influence of neutrophil/lymphocyte ratio on prognosis in mushroom poisoning". In: *Acta Med Mediterr* 30, pp. 849–864.
- Leshner, S (1967). "Compensatory Reactions in Intestinal Crypt Cells after 300 Roentgens of Cobalt-60 Gamma Irradiation". In: *Radiation Research* 32.3, p. 510.

- Liu, X et al. (2016). “Prognostic significance of neutrophil-to-lymphocyte ratio in patients with sepsis: A prospective observational study.” In: *Mediators Inflamm* 2016.
- Lord, JM et al. (2014). “The systemic immune response to trauma: an overview of pathophysiology and treatment.” In: *Lancet (London, England)* 384 (9952), pp. 1455–1465.
- Luo, M et al. (2007). “Are plasma citrulline and glutamine biomarkers of intestinal absorptive function in patients with short bowel syndrome?” In: *Journal of Parenteral and Enteral Nutrition* 31.1, pp. 1–7.
- Maciã I Garau, M, A Lucas Calduch, and EC López (2011). “Radiobiology of the acute radiation syndrome.” In: *Reports of practical oncology and radiotherapy : journal of Greatpoland Cancer Center in Poznan and Polish Society of Radiation Oncology* 16 (4), pp. 123–130.
- Magnotti, L and E Deitch (2005). “Burns, bacterial translocation, gut barrier function, and failure”. In: *The Journal of Burn Care & Rehabilitation* 26.5, pp. 383–391.
- Marck, RE et al. (2013). “Time course of thrombocytes in burn patients and its predictive value for outcome”. In: *Burns* 39.4, pp. 714–722.
- Margulis, L and D Bermudes (1985). “Symbiosis as a mechanism of evolution: status of cell symbiosis theory.” In: *Symbiosis (Philadelphia, Pa.)* 1. Grant numbers: NGR 004-025, pp. 101–124.
- Medzhitov, R (2008). “Origin and physiological roles of inflammation.” In: *Nature* 454 (7203), pp. 428–435.
- Mettler, FA (2001). *Medical management of radiation accidents*. Ed. by IA Gusev, AK Guskova, and FA Mettler. 2nd. CRC Press, Boca Raton, pp. 211–222.
- Millage, K and D Crary (2016). *Probability of mortality within 48 hours from radiation alone*. Tech. rep. DTRA-TR-16-011. Applied Research Associates, Inc.
- Moreau, D et al. (2007). “Platelet count decline: an early prognostic marker in critically ill patients with prolonged ICU stays”. In: *CHEST Journal* 131.6, pp. 1735–1741.
- Nathan, C and A Ding (2010). “Nonresolving inflammation.” In: *Cell* 140 (6), pp. 871–882.
- Oldson, D, J Wentz, and D Stricklin (2015). *HENRE 2.0 technical reference manual*. Tech. rep. DTRA-TR-15-070.
- Ossetrova, NI et al. (2014). “Early-response biomarkers for assessment of radiation exposure in a mouse total-body irradiation model.” In: *Health Phys* 106.6, pp. 772–786.
- Oughterson, A and S Warren (1956). *Medical effects of the atomic bomb in Japan*. (pp. 105). National Nuclear Energy Series VIII-8. New York: McGraw-Hill.
- Palmer, JL et al. (2011). “Development of a combined radiation and burn injury model”. In: *Journal of Burn Care & Research* 32.2, pp. 317–323.
- Pappas, PA et al. (2002). “Serum citrulline as a marker of acute cellular rejection for intestinal transplantation”. In: *Transplantation proceedings*. Vol. 34. Elsevier, pp. 915–917.
- Piton, G et al. (2010). “Plasma citrulline kinetics and prognostic value in critically ill patients”. In: *Intensive Care Medicine* 36.4, pp. 702–706.
- Piton, G et al. (2011). “Acute intestinal failure in critically ill patients: is plasma citrulline the right marker?” In: *Intensive Care Medicine* 37.6, pp. 911–917.
- Piton, G et al. (2013). “Enterocyte damage in critically ill patients is associated with shock condition and 28-day mortality”. In: *Critical Care Medicine* 41.9, pp. 2169–2176.
- Potten, Christopher S. (2004). “Radiation, the ideal cytotoxic agent for studying the cell biology of tissues such as the small intestine”. In: *Radiation Research* 161.2, pp. 123–136.

- Rhoads, JM et al. (2005). “Serum citrulline levels correlate with enteral tolerance and bowel length in infants with short bowel syndrome”. In: *The Journal of Pediatrics* 146.4, pp. 542–547.
- Riché, F et al. (2015). “Reversal of neutrophil-to-lymphocyte count ratio in early versus late death from septic shock.” In: *Crit Care* 19.
- Rimando, J et al. (2016). “The pretreatment neutrophil/lymphocyte ratio is associated with all-cause mortality in black and white patients with non-metastatic breast cancer.” In: *Front Oncol* 6.
- Saeed, M et al. (2011). “Multiparameter Intelligent Monitoring in Intensive Care II: A public-access intensive care unit database”. In: *Critical Care Medicine* 39.5, pp. 952–960.
- Saliccioli, JD et al. (2015). “The association between the neutrophil-to-lymphocyte ratio and mortality in critical illness: an observational cohort study.” In: *Crit Care* 19.
- Salman, T et al. (2016). “Prognostic value of the pretreatment neutrophil-to-lymphocyte ratio and platelet-to-lymphocyte ratio for patients with neuroendocrine tumors: An Izmir Oncology Group study.” In: *Chemotherapy* 61.6, pp. 281–286.
- Seok, J et al. (2013). “Genomic responses in mouse models poorly mimic human inflammatory diseases.” In: *Proceedings of the National Academy of Sciences of the United States of America* 110 (9), pp. 3507–3512.
- Serhan, CN, PA Ward, and DW Gilroy (2010). *Fundamentals of inflammation*. Cambridge University Press.
- Stavem, P et al. (1985). “Lethal acute gamma radiation accident at Kjeller, Norway: Report of a case”. In: *Acta Radiologica: Oncology* 24.1, pp. 61–63.
- Strauss, R et al. (2002). “Thrombocytopenia in patients in the medical intensive care unit: bleeding prevalence, transfusion requirements, and outcome”. In: *Critical care medicine* 30.8, pp. 1765–1771.
- Stricklin, D. (2013a). *Estimation of radiation permeability parameters for integration into the CSM model*. Tech. rep. ARA/HS-TN-13-012. Applied Research Associates, Inc.
- Stricklin, D (2013b). *Estimation of radiation permeability parameters for integration into the CSM model*. Tech. rep. ARA/HS-TN-13-012. Applied Research Associates, Inc.
- (2015). *Selection of a dose response relationship for radiation lethality with treatment for implementation in HENRE*. Tech. rep. DTRA-TR-15-007. Applied Research Associates, Inc.
- (2016). *Selection of demographic modification factors for radiation lethality for implementation in HENRE: Age and Gender*. Tech. rep. ARA/HS-TN-16-001. Applied Research Associates, Inc.
- Su, L et al. (2015). “Dynamic changes in amino acid concentration profiles in patients with sepsis”. In: *PloS one* 10.4, e0121933.
- Taneja, N et al. (2004). “A prospective study of hospital-acquired infections in burn patients at a tertiary care referral centre in North India”. In: *Burns* 30.7, pp. 665–669.
- The medical aspects of radiation incidents* (2013). Radiation Emergency Assistance Center/Training Site REACT/TS.
- Vaishnavi, C (2013). “Translocation of gut flora and its role in sepsis”. In: *Indian Journal of Medical Microbiology* 31.4, pp. 334–342.
- Valente, M et al. (2015). “Revisiting biomarkers of total-body and partial-body exposure in a baboon model of irradiation”. In: *PLoS One* 10.7, e0132194.

- Valparaiso, A et al. (2015). “Modeling acute traumatic injury”. In: *Journal of Surgical Research* 194.1, pp. 220–232.
- Vanderschueren, S et al. (2000). “Thrombocytopenia and prognosis in intensive care”. In: *Critical care medicine* 28.6, pp. 1871–1876.
- Wentz, J, D Oldson, and D Stricklin (2014a). *Mathematical models of human hematopoiesis following acute radiation exposure*. Tech. rep. DTRA01-03-D-0014. Applied Research Associates, Inc.
- (2014b). “Modeling the thrombopoietic effects of burn”. In: *Letters in Biomathematics* 1.1, pp. 111–126.
- (2015a). *Models of hematopoietic dynamics following burn for use in combined injury simulations*. Tech. rep. HDTRA1-14-D-003; 0005. Nuclear Survivability and Forensics Integrated Program Team.
- Wentz, J. M. et al. (2015b). “Mathematical model of radiation effects on thrombopoiesis in rhesus macaques and humans”. In: *Journal of Theoretical Biology* 383, pp. 44–60.
- Wijnands, K et al. (2015). “Arginine and citrulline and the immune response in sepsis”. In: *Nutrients* 7.3, pp. 1426–1463.
- Wolf, SE et al. (1999). “Cutaneous burn increases apoptosis in the gut epithelium of mice”. In: *Journal of the American College of Surgeons* 188.1, pp. 10–16.
- Youden, W (1950). “Index for rating diagnostic tests”. In: *Cancer* 3.1, pp. 32–35.
- Zahorec, R (2001). “Ratio of neutrophil to lymphocyte counts—rapid and simple parameter of systemic inflammation and stress in critically ill.” In: *Bratisl Lek Listy* 102.1, pp. 5–14.

## 8 Abbreviations, Acronyms and Symbols

ARA	Applied Research Associates, Inc.
ARDS	Acute respiratory distress syndrome
ARS	Acute radiation syndrome
AUC	Area under the curve
CI	Combined injury
d	Days
DAMP	Damage-associated molecular pattern
DTRA	Defense Threat Reduction Agency
GI-ARS	Gastrointestinal acute radiation syndrome
Gy	Gray
H-ARS	Hematopoietic acute radiation syndrome
HENRE	Health Effects from Nuclear and Radiological Environments
ICU	Intensive care unit
IND	Improvised nuclear device
MLT	Midline tissue
MIMIC	Multiparameter Intelligent Monitoring in Intensive Care
MODS	Multiple organ dysfunction syndrome
NLR	Neutrophil:lymphocyte ratio
PAMP	Pathogen-associated molecular pattern
PAMM	Platelet Attenuation Mortality Model
ROC	Receiver operating characteristic
ROS	Reactive oxygen species
SBS	Short bowel syndrome
SIMM	Small Intestine Mortality Model
WMD	Weapons of mass destruction
% TBSA	Percent of total body surface area

# A Small Intestine Model Update

In this appendix, we describe the determination of the parameters of the small intestine model related to burn response,  $a_0$ ,  $b_0$ ,  $k$ ,  $a_1$ ,  $b_1$ , and  $\Delta_b$ . The burn response in this report has been updated from the version described in Bellman and Stricklin, 2016. We make the following assumptions when fitting the model to data from Carter et al., 2014 and Jeschke et al., 2007:

- The post-insult villus cell data normalized to pre-insult levels is the same for rodents and humans. This is supported by the fact that the human and murine models report similar normalized villus nadirs following radiation.
- The time scale for suppression of villus cell proliferation is rescaled, based on the relative time difference between human and murine nadirs following acute 5 Gy radiation doses.

With the above assumptions, the burn model parameters were re-fit using the optimization method described in Bellman and Stricklin, 2016, with an adjustment to the cost function. A penalty has been added to the cost function when the nadirs of the simulations (time and value) do not match the timing and value of the minimum data points for each experiment. This penalty prevents a rapid decrease to the nadir immediately after the insult. An updated set of burn parameter values is provided in Table A.1, and an updated matrix of combined injury response is presented in Figure A.1.

Table A.1: Biological descriptions, parameters and variables for burn response in the small intestine mathematical model.

Parameter	Biological Description	Updated Value
$a_0$	Determines duration of burn effect on villus death	0.33 d <sup>-1</sup>
$b_0$	Describes maximum effect on villus death	0.36
$a_1$	Determines duration of burn effect on proliferation	0.0005 d <sup>-1</sup>
$b_1$	Describes maximum effect of burn on proliferation	0.15
$k$	Activation threshold for burn effect	18.83 %TBSA
$\Delta_b$	Delay after burn before proliferation suppression	3.84 d

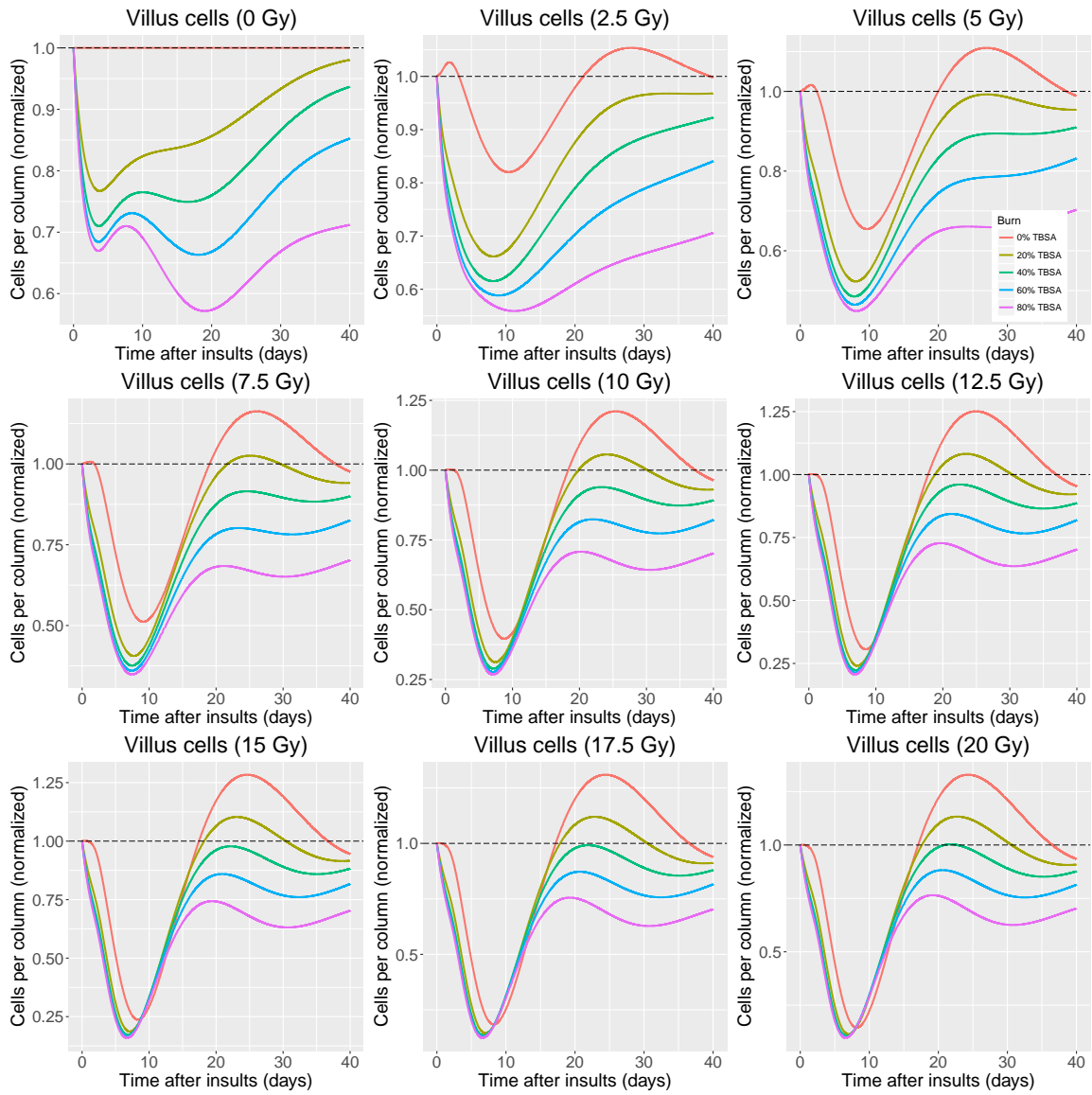


Figure A.1: Small intestine combined injury villus response with updated burn parameters (Table A.1).